Development and Characterization of a Functional Smart PVA/NC/PCL Nano-biocomposite Using E. Coli Phage: Insights into Physicochemical Properties and Antimicrobial Activity

Malahat Safavi[1], Reza Rezaei Mokarram[1*], Mahmood Sowti Khiabani[1], Alireza Ostad Rahimi[2], Abolfazl Barzegar[3]

1. Department of Food Industry Science and Engineering, Faculty of Agriculture, University of Tabriz, Iran.

2. Nutrition Research Center, Department of Clinical Nutrition, School of Nutrition& Food Sciences, Tabriz University of Medical Sciences, Tabriz, Iran.

3. Research Institute for Fundamental Sciences (RIFS), University of Tabriz, Tabriz, Iran.

Received Data: 6 January 2025
Revised Data: 6 February 2025
Accepted Data: 6 February 2025

Please cite this article as Malahat Safavi, Reza Rezaei Mokarram, Mahmood Sowti Khiabani, Alireza Ostad Rahimi, Abolfazl Barzegar., Development and Characterization of a Functional Smart PVA/NC/PCL Nano-biocomposite Using E. Coli Phage: Insights into Physicochemical Properties and Antimicrobial Activity., ***Innovative Food Technologies*** *(2025).*

Doi: https://doi.org/10.22104/ift.2025.7326.2193

This is a PDF file of an article that has undergone enhancements after acceptance, such as the addition of a cover page and metadata, and formatting for readability, but it is not yet the definitive version of record. This version will undergo additional copyediting, typesetting and review before it is published in its final form, but we are providing this version to give early visibility of the article. Please note that, during the production process, errors may be discovered which could affect the content, and all legal disclaimers that apply to the journal pertain.

© 2024 The Author(s). Published by irost.org.

* **corresponding author:** rmokarram@tabrizu.ac.ir

Journal Pre-proofs

Abstract:

Food packaging plays a critical role in preserving the freshness and quality of foods while preventing microbial spoilage. Advances in this field have led to the development of intelligent and active packaging systems incorporating nanotechnology. Among these, electrospinning has gained attention for producing nanofibrous materials with high surface-to-volume ratios, enabling the efficient loading of active agents.

In response to the growing concern over antibiotic-resistant bacteria, this study investigates the use of bacteriophages as an alternative antimicrobial agent. Lytic bacteriophages targeting Escherichia coli were isolated from Caspian seawater and immobilized onto electrospun nanofibers composed of polyvinyl alcohol (PVA), polycaprolactone (PCL), and bacterial nanocellulose (BNC). SEM confirmed successful phage immobilization, while TEM revealed their classification within the Siphoviridae and Podoviridae families.

The addition of PCL to PVA enhanced the fibers' mechanical strength, reduced defects, and improved water resistance. Incorporating BNC further strengthened the nanofiber structure and enhanced its matrix properties. Antimicrobial testing using the disc diffusion method revealed an inhibition halo of 13 mm, exceeding that of the antibiotic ampicillin. Notably, the functionalized nanofibers retained antimicrobial efficacy for up to one month, with stable phage viability at 24°C, 4°C, and -20°C.

These findings demonstrate the potential of electrospun nanofibers functionalized with bacteriophages as a sustainable solution for combating bacterial contamination in food packaging, contributing to enhanced food safety and extended shelf life.

Key Words:

Bacteriophages; Electrospinning; Polycaprolactone; Poly Vinyl Alcohol; Nanofiber; Bacterial Nanocellulose.

Journal Pre-proofs

1. Introduction

Active packaging, a cutting-edge technology, integrates antimicrobials, antioxidants, and moisture-absorbing agents into polymeric materials, effectively extending the shelf life of perishable products. Within this realm, electrospun nanofibers have gained prominence for their high porosity, substantial surface-to-volume ratio, flexibility, and superior loading capacity, making them particularly suitable for active packaging [1]. Polyvinyl alcohol (PVA), selected for its synthetic, non-toxic, and water-soluble nature, exhibits robust thermal stability and excellent mechanical properties [2].

The imperative exploration of alternative antibacterial treatments has arisen as a critical strategy to counter antibiotic overuse and effectively combat drug-resistant bacterial infections. In this context, using phage, among various options such as antibodies, probiotics, and antimicrobial peptides, stands out as a prominent antibacterial approach [3]. Bacteriophages (phages), being viruses capable of infecting and eliminating bacteria without affecting human or animal cells, have showcased remarkable bactericidal efficacy in numerous research studies [4-6]. Recent advancements in bio-nanotechnology have further harnessed the potential of phages as innovative functional nano-materials, finding applications in tissue regeneration materials and active food packaging [7].

The utilization of cellulose nanocrystals (CNC) as reinforcing materials enhances both the mechanical and thermal properties of nanofibers, contributing to improved nanofiber morphology and reduced diameters [8]. CNC-based nanofillers have demonstrated a remarkable ability to improve the mechanical and antibacterial properties of polymer matrices, such as PVA composites, making them promising candidates for active packaging applications [9]. These nanocrystals, with their nanometric dimensions, impressive strength, and biodegradability from renewable sources, facilitate the production of bio-based nanofibers with enhanced performance [10].

Journal Pre-proofs

In the pursuit of effective nanofiber fabrication, Polycaprolactone (PCL) emerges as a promising choice due to its semi-crystalline hydrophobic nature and excellent hemo compatibility. Despite its FDA-approved status, PCL electrospun membranes face durability challenges [11].

A novel surface modification technique involving the predrying of PVA and electrospinning hydrophobic PCL nanofibers has proven to significantly enhance the physical and mechanical properties of the resulting PVA/PCL composites [12]. Addressing these challenges necessitates an advanced strategy—leveraging a combination of polymers in the electrospinning process to mitigate individual weaknesses and enhance overall nanofiber performance. The study focuses on *Escherichia coli* (*E. coli*), a gram-negative bacillus in the *Enterobacteriaceae* family responsible for various human infections. [13]. Its transmission to humans occurs through multiple pathways, with contaminated foods playing a significant role [14, 15]. Ensuring the quality of these products through production, packaging, and distribution stages is imperative. The emergence of antibiotic resistance in bacteria further emphasizes the need for preventive measures against food contamination. Incorporating controlled amounts of antimicrobial substances into packaging materials can extend the shelf life of food, aligning with consumer preferences for natural preservatives [16]. Bacteriophages, harmless bacterial parasites, emerge as a viable solution for controlling pathogenic bacteria at every stage of food production. However, challenges in the utilization of phages, such as deactivation during food processing and the risk of bacterial resistance, underscore the importance of incorporating lytic phages into food packaging [17].

One approach involves immobilizing lytic phages on the surface of packaging material, facilitating their interaction with host cells on the food surface. [18].

The primary objective of this study was to design and fabricate a two-layer nanofiber packaging system using PCL and PVA-based electrospun materials. PVA, chosen as the primary

Journal Pre-proofs

component of the packaging, was selected for its excellent mechanical properties and non-toxic nature, ensuring the safety of the packaging for food contact applications. Additionally, a layer of PCL was incorporated into the median layer to enhance the mechanical strength of the fibers further. The results of this study not only contribute to the understanding of electrospinning as a method for encapsulating bacterial viruses but pave the way for advancements in phage-based active food packaging technology.

2. Materials and Methods

2-1. Materials

Escherichia coli (*E. coli* O157:H7) was procured from the microbial collection of the Department of Microbiology and the Applied Pharmaceutical Research Center at Tabriz University of Medical Sciences. The specific lytic phage of *E. coli* was isolated from the coastal waters of the Caspian Sea using Liu et al.'s method [19]. Bacterial nanocellulose was synthesized following the method outlined by Mahdieh Salari et al [20]. Polyvinyl alcohol (PVA) with a hydrolysis degree of 87-89% and a molecular weight of 146-186 kDa, along with polycaprolactone (PCL) with a molecular weight of 80,000, were acquired from Sigma-Aldrich. The SM buffer (composed of 5/8 g NaCl, 2 g MgSO4, 50 ml 1 M Tris-HCl, and 5 mL of a 2 wt% gelatin solution) was sourced from Merck, Germany. Nutrient Broth (NB), Muller Hinton Agar (MHA), and Luria Bertani (LB) culture media were obtained from Merck, Germany. All other chemicals and reagents utilized in the study were of analytical grade.

2-2. Methods

2-2-1. Preparation of Bacterial Nanocellulose

Bacterial nanocellulose pellicles were synthesized using "*Acetobacter xylinus*" in a molasses medium. For purification, the pellicles were washed with distilled water and treated with a 0.2 M NaOH aqueous solution at 90 °C for 30 min. The treated pellicles were then rinsed multiple times until neutralized. The purified BC pellicles were mechanically chopped into a cellulosic

Journal Pre-proofs

paste using a laboratory blender (Model 51BL32, Waring Co., USA) at 3500 rpm for 30 minutes.

To produce bacterial cellulose nanocrystals, the cellulosic paste was hydrolyzed with 98% sulfuric acid (50% w/w) at 50 °C for 40 minutes under vigorous stirring. The reaction was halted by diluting the suspension with approximately 10 times its volume of distilled water. The mixture was then centrifuged at 4000 g several times to concentrate the cellulose crystals and remove excess sulfuric acid. The sediment was collected and dialyzed against distilled water until a constant neutral pH was achieved.

Subsequently, mechanical treatment was performed through sonication in an ultrasonic bath (AS ONE, USD 4R, Japan) for 10 minutes at 40 kW while cooling in an ice bath. This was followed by homogenization using a high-shear homogenizer (Heidolph Silent Crusher M, Germany) at 18000 rpm for 1 hour [21]. The resulting aqueous suspension, containing approximately 0.8% (w/w) cellulose nanocrystals, was stored in a refrigerator at 4 °C for future use.

2-2-2. Preparing Electrospinning Solutions

The electrospinning solutions were meticulously prepared in two distinct steps. Initially, 10 g of PVA powder was dissolved in 100 mL of preheated water and vigorously mixed for 4 hours to ensure complete dissolution. Subsequently, 2.5, 5, and 7.5 g of BNC powder was meticulously added to the solution, creating a homogeneous mixture.

In the second step, a solution for electrospinning was prepared by dissolving 15 g of PCL powder in 100 ml of dichloromethane solvent. The solution was meticulously mixed for 30 min to achieve the desired consistency and homogeneity.

2-2-3. Bacterial Strain Preparation and Specific Lytic Phage Activation

Journal Pre-proofs

The bacteriophage strain originated from the coastal waters of the Caspian Sea. Seawater was filtered through 0.22-micrometer pore-size membranes, and the presence of phages was assessed using the two-layer agar method to visualize plaques [19]. Lyophilized *Escherichia coli* bacteria were aseptically reconstituted in a laminar flow hood, breaking the vial under sterile conditions. Subsequently, 0.5 mL of sterile Nutrient Broth (NB) culture medium was added using a sampler to create a bacterial suspension. This bacterial suspension was then transferred to Luria Bertani (LB) solid culture medium until reaching to 0.5 McFarland concentration and incubated at 37°C for 24 hours [22]. The LB culture medium was initially enriched with calcium chloride to activate the specific phage. Phage multiplication was facilitated using the double-layer agar method, and the positive plates were stored at 4°C for preservation [18].

2-2-4. Electrospinning Process

The electrospinning process was conducted utilizing the ES1000 model electrospinning machine, manufactured by Fannavaran nanomeghyas Company in Iran. Equipped with a drum collector, this advanced machine facilitated the creation of nanofiber mats with precision. The electrospinning process was conducted for 30 minutes under controlled conditions, including a distance of 16 Cm, drum speed of 200 RPM, nozzle angle of 90°, flow rate of 2 mL/hr, and a high voltage supply of 24 KV. The electrospinning process was conducted using a dual-nozzle setup. One nozzle was dedicated to electrospinning PCL, while the other delivered a composite solution of PVA, BNC, and phages. Both nozzles were equipped with stainless-steel No. 18 blunt-ended needles to ensure precise solution delivery. The dual-nozzle configuration allowed for the simultaneous deposition of distinct materials, facilitating the fabrication of hybrid nanofibrous structures. These optimized conditions ensured the successful fabrication of nanofiber mats with uniform morphology and desired properties for effective active packaging applications.

Journal Pre-proofs

2-2-5. Immobilization of Phage on Electrospun Fibers within a PCL/PVA/BNC

To immobilize the phage, electrospinning was employed by incorporating a bacteriophage suspension into a polymeric solution. Specifically, 5 mL of a phage solution (with a concentration of approximately 10^{10} PFU/mL) was introduced into the PVA solution contain different concentrations of BNC. The resulting suspension underwent electrospinning under optimal conditions, and upon the formation of nanofibers, it was left at room temperature for a duration of 24h [23].

2-2-6. Scanning Electron Microscope Imaging to Verification Nanocellulose Matrix

Verification of phage immobilization on the electrospun fibers was conducted through SEM imaging (Model MIRA3 FEG-SEM, Tescan, Czech Republic). Prior to imaging, the fibers were coated with a layer of gold for 5 minutes. Image analysis was performed using a system with a 26-kW voltage acceleration [24].

2-2-7. Morphological Examination of Bacteriophages using Transmission Electron Microscopy (TEM)

For the morphological investigation of bacteriophages, ten microliters of the bacteriophage suspension were deposited onto a grid coated with carbon and left to dry at room temperature. Subsequently, negative staining was performed using a 2% uranyl acetate solution. The stained grids were then examined using a transmission electron microscope (LE0906: Zeiss, Germany), and images of the targeted areas were captured with a camera (Gatan Multiscan 791 CCD Camera).

2-2-8. Water Absorption, Water Content, Water Solubility and Water Contact Angle Measurements

To assess the water absorption capacity of the optimized fabricated fibers, 2 x 2 cm pieces of various fibers were initially weighed and placed in a desiccator with 0% humidity, achieved

Journal Pre-proofs

using calcium sulfate, to dehydrate them. Subsequently, the fibers were transferred to a desiccator set at 55% relative humidity, maintained with a saturated calcium nitrate solution, until they reached equilibrium weight. The moisture absorbance rate was calculated using the equation 1:

Equation. 1

For the determination of water content, 2 x 2 cm pieces of the fibers were sectioned and placed in a desiccator at 55% relative humidity overnight, followed by weighing. Afterward, the samples were dried in an oven at 105°C for 6 hours, cooled in the desiccator, and weighed again. The water content was then calculated using the equation 2:

Equation. 2 $$\text{Water Content } (\%) = \frac{\text{Initial Weight} - \text{Final Weight}}{\text{Initial Weight}} \times 100$$

For assessing water solubility, 100 mg of each fiber, previously dried in an oven at 105°C, was immersed in 50 mL of water and agitated for 6 hours at room temperature. After incubation, the fiber solut $\text{Solubility Rate } (\%) = \frac{\text{Weight of Insoluble Residue}}{\text{Initial Weight}} \times 100$ before weighing. The solubility rate was determined using the equation 3:

Equation. 3:

The dynamic water contact angle was utilized to delve deeper into the water absorption behavior of the mats. This assessment was conducted using a G10 device manufactured by KRUSS Germany, known for its precision and reliability in measuring surface interactions with liquids.

2-2-9. Fourier Transform Infrared Spectroscopy (FTIR):

To elucidate the chemical structure and interactions among the components, Fourier Transform Infrared (FTIR) spectroscopy was conducted over the range of 4000–400 cm^{-1} (Tensor 27, Bruker, Germany). FTIR spectra were acquired with a resolution of 4 cm^{-1} and an average of 256 scans per spectrum. All measurements were performed at room temperature and reported

based on transmission. An empty KBr disc served as the reference, and its spectrum was subtracted from the sample spectrum to eliminate spectral artifacts arising from KBr impurities and water [25].

2-2-10. X-ray Diffraction (XRD) Analysis:

The X-ray diffraction (XRD) analysis of films was conducted using a Bruker D5000 instrument (Siemens, Germany) equipped with CuKα radiation (wavelength = 0.154 nm). The system was operated at 40 kV and 30 mA. Measurements were performed at room temperature over a 2θ range of 5° to 50°, with a step size of 0.05° and a scanning speed of 1° per minute [21].

2-2-11. Thermal Analysis:

The thermal properties of the films were assessed using Differential Scanning Calorimetry (DSC) (F3 200 DSC, Netzsch, Germany). Film samples were cut into small pieces and placed on a sample pan within the DSC equipment, with an empty pan serving as the reference. The melting point (Tm) of the different films was determined via heating scans conducted at a rate of 10 °C/min from 30 °C to 250 °C under a constant flow of nitrogen gas [21].

2-2-12. Mechanical Properties Analysis

The mechanical properties, including Ultimate Tensile Strength (UTS), Young's Modulus (YM), and Strain to Break (SB), of the films were assessed following the ASTM standard method D882-91 (ASTM, 1996). Initially, the samples underwent a conditioning period of 24 hours at a relative humidity of 57%. Subsequently, each film was precisely cut into a dumbbell shape, measuring (8 cm × 0.5 cm), and securely positioned between two grips of the testing machine. The primary grip breaking and cross-head speed were meticulously set at 50 mm and 5 mm/min, respectively, ensuring consistent and accurate measurements [21].

2-2-13. Evaluation of Antimicrobial Activity, Phage Plaque Observation, and Titer Determination

Journal Pre-proofs

half McFarland's concentration of *E.coli* bacteria were cultured in an LB liquid medium at 37°C for 24 hours. Afterward, 100 µL of the host bacteria were mixed with 5 mL of semi-solid LB medium and then spread onto an LB agar plate. Following a 15-minute stabilization period, a serial dilution of the phage was prepared. 10 µL of the diluted phage solution was added to the surface of the actively growing bacterial culture, ensuring an even distribution across the plate. The plates were incubated overnight at 37°C. The appearance of plaques the following day indicated the phage's ability to lyse the host bacteria. The number of phage particles in the suspension was quantified by counting the plaques and using the following equation 4:

Equation. 4: $\text{Determination of Phage Number (PFU/mL)} = (\frac{\text{Number of plaques}}{\text{Dilution factor}}) \times$ Volume of phage solution plated (mL) [26].

2-2-14. Assessment of the Antimicrobial Activity of Nano BioComposite

The antimicrobial effect of the electrospun active nanofibers was examined using the disk diffusion method. Initially, discs with a 6-mm diameter were crafted from electrospun active fibers of PCL/PVA/BNC/bacteriophage. These discs were then positioned on a plate containing Muller Hinton Agar (MHA) culture medium, previously inoculated with a suspension of *Escherichia coli* bacteria at a concentration of 10^{10} CFU/mL. Nanofibers without the phage served as the negative control, while a disc containing ampicillin was selected as the positive control. Subsequently, the plates were incubated at 37°C for 24 hours, and the zone of inhibition was determined by measuring the diameter of the inhibition zone [27].

2-2-15. Assessment of the Antimicrobial Efficacy of Immobilized Phages Over Time

To evaluate the sustained antimicrobial efficacy of phages immobilized on electrospun fibers over a one-month period, active nanofibers were securely stored in an airtight container at room temperature (25°C). To maintain a relative humidity of 80-86%, saturated barium chloride was employed. The host bacterium underwent incubation at 37°C for 24 hours. Subsequently, a bacterial suspension was prepared with a dilution of 10^3 CFU/mL, and 2 Cm diameter slices

Journal Pre-proofs

were extracted from both active and control nanofibers. These slices were immersed in 9 mL of the bacterial suspension. The bacterial count in the suspension was determined through seven tests conducted on days 1, 5, 10, 15, 20, 25, and 30, following the storage of active and control nanofibers.

2-2-16. Statistical analysis

All experiments conducted in this research were replicated three times consecutively. Statistical analysis was performed using both the One-way and Two-way analysis of variance (ANOVA) methods, followed by multiple comparisons between individual datasets through the Tukey honest significant difference test (GraphPad Prism, version 9, San Diego, CA). A significance threshold of $P < 0.05$ was applied.

3. Results and Discussion

3.1. Physical properties

3.1.1. Moisture Content, Water Solubility, and Water Absorption

Figure 1 presents a comparative analysis of the moisture content, water solubility, and water absorption characteristics for PVA, PCL, PVA-PCL, and PVA-PCL with varying concentrations of nanocellulose (NC). The results highlight significant differences in these properties influenced by the material composition and the inclusion of NC. As shown in Figure 1a, moisture content increases significantly with the incorporation of NC into the PVA-PCL matrix. Among the samples, PVA exhibits the highest moisture content, indicative of its strong hydrophilic nature. The addition of NC to PVA-PCL at increasing concentrations (2.5%, 5%, and 7.5%) further enhances the moisture content, with the PVA-PCL-NC (7.5%) showing the highest values. This suggests that NC, due to its hydrophilic properties, increases the water-attracting capability of the composite. Similar trends of hydrophilic reinforcement by NC were noted in other polymer matrices [28]. PCL, a hydrophobic polymer, shows the lowest moisture content, demonstrating its inherent resistance to water uptake [29]. The data in Figure 1b reveal

Journal Pre-proofs

a decreasing trend in water solubility as NC concentration increases in PVA-PCL composites. PVA alone exhibits the highest solubility, while PCL demonstrates minimal solubility due to its hydrophobic nature. The PVA-PCL combination shows intermediate solubility, which is progressively reduced with the incorporation of NC. This decrease suggests that NC enhances the crystalline structure and crosslinking density of the composite, reducing its solubility in water [30]. The results in Figure 1c show that the incorporation of NC significantly reduces water absorption in PVA-PCL composites. While PVA-PCL alone exhibits the highest water absorption, the addition of NC at increasing concentrations (2.5%, 5%, and 7.5%) systematically decreases the absorption capacity. This is likely due to the ability of NC to reinforce the polymer matrix, creating a denser and less porous structure that limits water penetration. PCL, again, demonstrates minimal water absorption, aligning with its hydrophobic characteristics [31].

The results clearly demonstrate the influence of NC on moisture-related properties of the PVA-PCL matrix. The addition of NC increases the overall moisture content due to its hydrophilic nature, but simultaneously reduces water solubility and absorption by reinforcing the matrix structure. This dual behavior highlights NC's role as both a hydrophilic agent and a structural reinforcer [28].

At higher NC concentrations, the enhanced crystallinity and barrier properties of the composite materials are particularly notable. These improvements could be advantageous in applications where controlled water interaction and stability are critical, such as in biomedical scaffolds or food packaging [30]. Future studies could explore the effect of NC particle size and surface modifications on these properties for further optimization [31].

Figure 1. a) Moisture Content, b) Water Solubility, and c) Water Absorption of Nanofibers. Poly vinyl alcohol nanofibers (PVA), Polycaprolactone nanofibers (PCL), Poly vinyl alcohol + Polycaprolactone nanofibers (PVA-PCL), and Poly vinyl alcohol + Polycaprolactone + nanocellulose nanofibers (PVA-PCL-NC). The data, mean ± SD (n = 3), demonstrate the impact of formulations on cell cycle regulation and gene expression. NS: not significant, **p < 0.01, ****p < 0.0001, versus multiple comparisons.

Journal Pre-proofs

3.1.2. Surface hydrophobicity

As shown in Figure 2, the surface hydrophobicity of the electrospun nanofibers was evaluated using contact angle measurements. This parameter provides critical insight into the wettability of the biocomposite surfaces, which directly affects their functionality in applications such as antimicrobial activity and biocompatibility.

The contact angle for PVA nanofibers was the lowest (46°), indicating a highly hydrophilic surface. This is attributed to the hydroxyl groups in the PVA structure, which promote water attraction. In contrast, PCL nanofibers exhibited the highest contact angle (140°), confirming their hydrophobic nature due to the absence of polar functional groups in their aliphatic polyester backbone.

The PVA-PCL blend nanofibers displayed an intermediate contact angle of 133°, indicating that the blending of PVA and PCL reduces the individual polymers' extreme hydrophilic and hydrophobic characteristics. The incorporation of bacterial cellulose (BC) and increasing concentrations of nanocellulose (NC) into the PVA-PCL matrix progressively reduced the contact angle. The values for PVA-PCL-NC composites were 104° for 2.5% NC, 78° for 5% NC, and 55° for 7.5% NC, demonstrating a significant increase in surface hydrophilicity with higher NC content.

The progressive reduction in contact angle with increasing NC concentration can be attributed to the hydrophilic nature of NC, which introduces additional hydroxyl groups to the composite surface, enhancing water-attracting properties. This trend is consistent with prior studies where NC was shown to modulate surface hydrophilicity in polymeric composites [32]. Furthermore, the enhanced hydrophilicity of the bio-composites is beneficial for biomedical applications, as it facilitates improved cell adhesion and biocompatibility [31].

The moderate hydrophobicity observed for the PVA-PCL blend without NC suggests potential for applications where controlled water interaction is required, such as water-resistant

Journal Pre-proofs

packaging. Conversely, the significant hydrophilicity achieved with PVA-PCL-NC (7.5%) indicates suitability for biomedical applications requiring strong interaction with aqueous environments, such as wound dressings and antimicrobial scaffolds. The tunable nature of the surface properties highlights the versatility of these bio-composites for diverse applications.

Figure 2. Contact angle measurements of PVA, PCL, PVA-PCL, and PVA-PCL-NC composites with varying concentrations of nanocellulose (2.5%, 5%, and 7.5%). Data are presented as mean ± SD (n = 3). Statistical significance: ns: not significant, **p < 0.01, **p < 0.0001.

3.2. Mechanical properties

Figure 3 illustrates the ultimate tensile strength (UTS) and strain to break (SB) for various nanofibers, including PVA, PCL, PVA-PCL blends, and PVA-PCL-NC composites with increasing concentrations of nanocellulose (NC). These parameters reveal how the mechanical performance of the materials is influenced by composition and the addition of NC.

The results show distinct variations in UTS across the tested groups. PVA exhibited a moderate UTS of 0.31 MPa, attributed to its inherent mechanical properties and hydrogen bonding between polymer chains. In contrast, PCL had the lowest UTS (0.16 MPa), reflecting its flexible and less rigid nature. The PVA-PCL blend demonstrated a slightly higher UTS (0.23 MPa) than PCL, but lower than pure PVA, indicating partial reinforcement from the blend but reduced performance due to the weaker mechanical properties of PCL.

The incorporation of NC significantly enhanced UTS in the PVA-PCL-NC composites. The UTS increased progressively with higher NC content, reaching 0.33 MPa at 2.5% NC, 0.39 MPa at 5% NC, and 0.45 MPa at 7.5% NC. This improvement can be attributed to NC's high stiffness and strength, which acts as a reinforcing agent by effectively transferring stress and improving the load-bearing capacity of the nanofiber matrix. Similar trends have been reported in other studies where NC addition improves the mechanical performance of polymer composites [33].

Journal Pre-proofs

For SB, PVA, PCL, and PVA-PCL exhibited similar strain values, reflecting limited elongation capability due to the inherent brittleness of PVA and the less elastic nature of the blend. However, the addition of NC significantly improved the SB of the nanofibers. At 2.5% NC, the SB increased substantially compared to PVA, PCL, and PVA-PCL fibers. Further increases in NC concentration (5% and 7.5%) maintained high SB values, highlighting the role of NC in enhancing flexibility by creating a robust yet elastic network within the matrix.

This increase in SB is likely due to the uniform dispersion of NC within the polymer matrix at lower concentrations, facilitating effective load distribution and preventing premature failure. However, at higher NC content (7.5%), SB remained stable, possibly due to the onset of agglomeration, which slightly reduces matrix mobility. These findings align with prior research, where CNC-enhanced polymer composites demonstrated improved tensile properties without significant trade-offs in elongation [34].

The mechanical properties of the nanofibers were significantly improved with the addition of NC, as evidenced by increased UTS and SB. These findings demonstrate the potential of PVA-PCL-NC composites for applications requiring enhanced strength and flexibility, such as tissue engineering scaffolds or antimicrobial membranes. Further optimization of NC concentration and dispersion can maximize mechanical performance.

Figure 3. Tensile properties of Polyvinyl alcohol (PVA), Polycaprolactone (PCL), PVA-PCL blends, and PVA-PCL nanocomposites with 2.5%, 5%, and 7.5% NC. Data represent mean ± SD (n = 3). Statistical significance: $p < 0.01$; ns = not significant.

3.3. FTIR

The Fourier Transform Infrared (FT-IR) spectra of pure polyvinyl alcohol (PVA), polycaprolactone (PCL), their blend (PVA-PCL), and nanocomposites with nanocellulose (PVA-PCL-NC at 5% and 7.5% NC content) are illustrated in Figure 4. The FT-IR analysis was conducted to investigate the chemical interactions and compatibility between the components of the nanocomposite system.

Journal Pre-proofs

In the spectrum of pure PVA, characteristic absorption bands were observed at ~3300 cm^{-1}, corresponding to the O–H stretching vibrations, indicating the presence of hydroxyl groups. The peaks at ~2940 cm^{-1} and ~2900 cm^{-1} can be attributed to the asymmetric and symmetric stretching vibrations of C–H bonds. Additionally, the sharp band at ~1700 cm^{-1} is indicative of C=O stretching, which may arise due to residual hydrolyzed acetate groups. The bands around ~1100 cm^{-1} represent C–O stretching vibrations, confirming the structure of PVA.

For the PCL spectrum, the characteristic peaks include the prominent absorption band at ~1720 cm^{-1}, corresponding to the stretching vibrations of the carbonyl (C=O) groups. The peaks at ~2930 cm^{-1} and ~2860 cm^{-1} represent asymmetric and symmetric C–H stretching vibrations of the aliphatic chain. The bands observed at ~1170 cm^{-1} and ~1295 cm^{-1} correspond to C–O–C stretching vibrations, typical of ester groups in PCL.

The FT-IR spectrum of the PVA-PCL blends exhibits absorption bands characteristic of both PVA and PCL, indicating the successful blending of the two polymers. The O–H stretching peak from PVA (~3300 cm^{-1}) slightly broadens, suggesting potential intermolecular hydrogen bonding between the hydroxyl groups of PVA and the carbonyl groups of PCL. The C=O stretching band at ~1720 cm^{-1} from PCL remains prominent, confirming the presence of the PCL component in the blend.

Several notable changes were observed in the FT-IR spectra for the nanocomposites containing nanocellulose (PVA-PCL-NC 5% and 7.5%). In both cases, the O–H stretching band (~3300 cm^{-1}) becomes broader and shifts slightly, indicating enhanced hydrogen bonding interactions between the nanocellulose, PVA, and PCL. The intensity of the C=O stretching band (~1720 cm^{-1}) increases with the addition of nanocellulose, suggesting the incorporation of nanocellulose into the polymer matrix and its interaction with the carbonyl groups of PCL.

Additionally, the presence of nanocellulose is evidenced by the enhancement of absorption bands in the fingerprint region. Peaks associated with C–O stretching vibrations (~1100 cm^{-1})

Journal Pre-proofs

exhibit increased intensity in the PVA-PCL-NC spectra compared to the pure polymers and the blend. This indicates the successful integration of nanocellulose, rich in hydroxyl groups, into the composite matrix.

Interestingly, at higher nanocellulose content (7.5%), the FT-IR spectrum shows a further increase in the intensity and broadening of the O–H and C=O bands, highlighting stronger intermolecular interactions. The increased intensity of the bands in the fingerprint region further confirms the reinforcement effect of nanocellulose within the polymer matrix.

In summary, the FT-IR analysis demonstrates the compatibility and interaction between PVA, PCL, and nanocellulose in the prepared nanocomposite fibers. Incorporating nanocellulose enhances hydrogen bonding and reinforces the composite structure, which is critical for the improved functional and antimicrobial properties of the PVA/BC/PCL nano-bio composite.

The implemented spectroscopic analytical approaches allowed for the chemical identification and visualization of the electrospun fiber mats. FT-IR spectroscopy was performed as a chemical analysis, and corresponding spectra confirmed the presence of unaltered polymer fibers with characteristic PVA-PCL bands as depicted by the PVA and PCL reference spectra [35].

The FT-IR results revealed enhanced hydrogen bonding with the incorporation of nanocellulose (NC), especially at higher NC content (7.5%), as evidenced by the broadening and intensification of the O–H and C=O stretching bands. These changes support the hypothesis of strong intermolecular interactions between PVA, PCL, and NC, contributing to the improved functional properties observed in PVA-PCL-NC composites. Comparatively, our findings align with previous studies, such as those by Ji, Xinbin, et al. (2021), who reported similar hydrogen bonding effects in PVA composites reinforced with cellulose nanocrystals. These interactions are critical in determining the chemical compatibility and stability of nanocomposite systems [36].

Journal Pre-proofs

Following the chemical analysis of electrospun fiber mats, the mechanical properties of the fiber networks were assessed. The mechanical performance of electrospun fiber mats is influenced by various factors, including fiber diameter, network architecture, and polymer selection. Additionally, collector rotation speeds may induce oriented fiber deposition, further impacting mechanical properties. Hence, uniaxial tensile testing was conducted parallel and perpendicular to the rotation direction of the collector to evaluate mechanical properties in both directions and detect any anisotropy resulting from fiber alignment [37].

Figure 4. represents the FT-IR spectrum of PVA) Poly vinyl alcohol nanofibers, PCL) Polycaprolactone nanofibers, PVA-PCL) Poly vinyl alcohol + Polycaprolactone nanofibers, and PVA-PCL-NC) Poly vinyl alcohol + Polycaprolactone + nanocellulose nanofibers (at different percentages).

3.4. XRD

The X-ray diffraction (XRD) patterns of PVA, PCL, PVA-PCL, and PVA-PCL-NC nanofibers with varying concentrations of nanocellulose (NC) (2.5%, 5%, and 7.5%) are presented in Figure 5. These results provide insights into the crystalline structures and interactions within the composite materials.

The XRD pattern of PVA nanofibers exhibited a broad diffraction peak around $2\theta = 19.5°$, confirming its semicrystalline nature. This peak arises from interchain hydrogen bonding in PVA, forming small crystalline domains dispersed within an amorphous matrix. These findings align with previous studies reporting the semicrystallinity of electrospun PVA fibers [38].

In contrast, PCL nanofibers exhibited sharp and well-defined peaks at $2\theta = 21.3°$ and 23.6°, corresponding to the (110) and (200) crystalline planes of PCL, respectively. These peaks highlight the highly crystalline nature of PCL, consistent with the regular packing of its polymer chains. Similar crystalline peaks have been observed in electrospun PCL nanofibers, attributed to their semicrystalline structure [39].

The XRD pattern of PVA-PCL nanofibers exhibited characteristic peaks of both PVA (broad peak at 19.5°) and PCL (sharp peaks at 21.3° and 23.6°). However, a slight reduction in the

Journal Pre-proofs

intensity of the PCL peaks was observed, suggesting partial disruption of PCL's crystalline domains due to interactions with PVA. This disruption may result from intermolecular interactions, such as hydrogen bonding or van der Waals forces, forming a more homogenous composite with intermediate crystalline behavior. Similar reductions in crystallinity have been reported in PVA-PCL blends due to polymer chain interactions [40]. Incorporation of nanocellulose into the PVA-PCL matrix altered the XRD patterns significantly.

At 2.5% NC concentration, the intensity of the PVA peak at 19.5° slightly increased, indicating that NC promotes hydrogen bonding and reinforces crystalline regions of PVA. The PCL peaks were retained but slightly diminished in intensity, suggesting minor disruption of PCL crystallinity. This finding aligns with prior research demonstrating that nanocellulose can act as a reinforcing filler in polymer matrices, enhancing the crystalline regions while maintaining structural integrity [41].

At 5% NC concentration, further reduction in the PCL peak intensity was observed, alongside broadening of the PVA peak. This trend suggests that increasing NC content disrupts the regular packing of both PVA and PCL chains, leading to a more amorphous composite. The enhanced amorphous nature can be attributed to better dispersion of NC, which interacts with the polymer chains and disrupts crystallinity.

At 7.5% NC concentration, a weak new peak emerged around $2\theta = 22.5°$, corresponding to the crystalline structure of nanocellulose. This confirms the incorporation of NC into the polymer matrix and its influence on the crystalline behavior of the composite. The broadening of peaks at this concentration suggests that NC further reduces polymer chain packing, improving uniformity but slightly decreasing overall crystallinity. These observations are consistent with other studies, where high NC concentrations reduced crystallinity due to nanofiller-polymer interactions [42].

Journal Pre-proofs

The observed decrease in crystallinity with increasing NC content supports findings from other researchers. For example, studies have shown that NC incorporation in PVA or PCL matrices disrupts polymer chain packing and enhances amorphous regions while reinforcing the matrix mechanically [43]. Moreover, the appearance of a nanocellulose crystalline peak (22.5°) highlights its successful integration, corroborating prior work showing that NC retains its crystallinity within composites, even at higher loadings [44].

The XRD analysis revealed that NC incorporation into PVA-PCL nanofibers altered their crystalline properties, with higher NC concentrations reducing crystallinity and enhancing amorphous regions. This structural modification highlights the potential of nanocellulose as a reinforcing agent in composite materials, balancing improved dispersion and mechanical properties with reduced crystallinity.

Figure 5. X-ray diffraction (XRD) analysis of Polyvinyl alcohol nanofibers (PVA), Polycaprolactone nanofibers (PCL), Polyvinyl alcohol + Polycaprolactone nanofibers (PVA-PCL), and Polyvinyl alcohol + Polycaprolactone + nanocellulose nanofibers at different percentages (PVA-PCL-NC).

3.5. Thermal properties

In the Figure. 6 the thermal properties of the prepared nanocomposite fibers—pure PVA, pure PCL, their blend (PVA-PCL), and PVA-PCL with varying nanocellulose (NC) concentrations (2.5%, 5%, and 7.5%)—were analyzed using differential scanning calorimetry (DSC) and thermogravimetric analysis (TGA). The obtained results are summarized below and compared with related studies in the field.

The DSC thermogram of pure PVA nanofibers showed a characteristic melting temperature (Tm) around 200°C, associated with its crystalline structure, while TGA indicated a two-stage decomposition process [45]. The first stage involved moisture evaporation at lower temperatures, and the second stage reflected the breakdown of the polymer backbone. Similarly, PCL nanofibers exhibited a melting temperature near 60°C, consistent with its semicrystalline nature, and a single degradation peak at higher temperatures, indicating its

Journal Pre-proofs

relatively higher thermal stability compared to PVA. These results align with prior studies that report similar thermal profiles for pure PVA and PCL polymers [45].

Thermal Properties of PVA-PCL Blend Nanofibers

The PVA-PCL blend nanofibers demonstrated combined thermal features of both PVA and PCL, with distinct melting points for each polymer. This dual behavior suggests a successful blending of the two polymers. The degradation onset temperature of the blend shifted higher compared to individual polymers, indicating improved thermal stability, likely due to enhanced intermolecular interactions between the polymer chains. Similar findings were reported by Zhang et al. (2019), who observed improved thermal stability in PVA-PCL blends due to synergistic interactions between the two polymers [46].

The addition of nanocellulose (NC) to the PVA-PCL matrix resulted in significant changes to the thermal properties. At 7.5% NC concentration, the TGA results showed a higher degradation onset temperature compared to the neat PVA-PCL blend, confirming that nanocellulose acts as a reinforcing agent. The thermal stability enhancement is attributed to the high thermal stability of NC, which restricts polymer chain mobility and delays decomposition. This observation agrees with the findings of Li et al. (2020), who reported similar enhancements in thermal stability upon incorporating nanocellulose into polymer matrices [47].

DSC results revealed a slight shift in melting temperatures and a reduction in the intensity of melting peaks with increasing NC content. This suggests a decrease in crystallinity due to the disruption of the polymer's regular chain alignment by NC, leading to a more amorphous structure. A similar reduction in crystallinity upon NC addition has been documented in other studies on nanocellulose-reinforced composites [48].

The observed improvements in thermal stability and the reduction in crystallinity in PVA-PCL-NC composites are consistent with the behavior of other polymer-nanocellulose systems. For

Journal Pre-proofs

instance, in PLA-based nanocellulose composites, researchers reported increased thermal stability and disrupted crystalline phases due to strong polymer-NC interactions [49]. These findings suggest that the incorporation of NC into PVA-PCL blends enhances thermal performance and alters the crystalline structure, potentially expanding their use in applications requiring thermal resistance.

The thermal analysis of PVA-PCL nanocomposite fibers with nanocellulose revealed a marked enhancement in thermal stability and modifications to the crystalline structure. At higher NC concentrations (7.5%), the composites exhibited optimal thermal properties, attributed to the reinforcing effects of nanocellulose.

Figure 6. Thermal properties of Poly vinyl alcohol nanofibers (PVA), Polycaprolactone nanofibers (PCL), Poly vinyl alcohol + Polycaprolactone nanofibers (PVA-PCL), and Poly vinyl alcohol + Polycaprolactone + nanocellulose nanofibers at different percentages (PVA-PCL-NC).

3.6. Microstructure

SEM images of the fabricated nanofibers are presented in Fig. 7, showcasing a diverse range of

compositions and structures. Figure 7a depicts pure PVA nanofibers, revealing a network of ultrafine fibers with random orientations. These fibers exhibit consistent diameters throughout the image, contributing to their uniform appearance.

In Fig. 7b, PCL nanofibers share similarities with PVA nanofibers but display slightly thicker fibers with a smoother, more uniform texture. The electrospinning of PVA blended with PCL (Fig. 7c) results in fibers that exhibit characteristics of both polymers, displaying a range of diameters and variations in surface smoothness.

The introduction of NC into the PVA-PCL nanofibers, as shown in Fig. 7d, introduces rougher, more textured areas, indicating the successful incorporation of nanocellulose within the nanofiber matrix. This modification alters the surface morphology, suggesting potential enhancements in properties such as mechanical strength and biocompatibility.

Journal Pre-proofs

Figure 7e demonstrates the successful immobilization of bacteriophages onto the nanofiber matrix. The presence of bacteriophages within the nanofibers is evident.Antimicrobial active food packaging demands stability of the bioactive cargo over prolonged storage periods while ensuring controlled and consistent release. Moreover, fiber packaging necessitates robust mechanical properties for practical application. Scanning electron microscopy was employed to examine the surface morphology of various fiber mats and to quantify individual fiber diameters. The electrospinning process yielded defect-free fibers with random orientation, essential for consistent fiber dissolution and subsequent bacteriophage release. This random orientation also enhances mechanical strength, enabling the packaging to withstand tensile forces in any direction during handling. The average fiber diameters ranged from 100 to 300 nm across all specimens, with a uniform size distribution, indicating reliable fabrication. Interestingly, PCL fibers exhibited slightly larger diameters than PVA fibers, but blending PCL with PVA reduced fiber size. Incorporating nanocellulose into PVA-PCL nanofibers resulted in a slightly rougher morphology, indicating successful nanocellulose integration. Notably, all fibers displayed uniformity without beads or anomalies. Figure 7f demonstrates effective bacteriophage immobilization within the fiber matrix. Analyzing the surface structure of fibers via electron microscopy was crucial, as fiber architecture influences bacteriophage preservation efficiency post-electrospinning [50].

Fig.7. SEM micrographs of the surfaces of (a) Poly vinyl alcohol (PVA) nanofiber, (b) Polycaprolactone (PCL) nanofiber, (c) PVA-PCL nanofiber, (d) PVA-PCL nanofiber containing nanocellulose (NC), (e) bacteriophages, (f) and bacteriophages containing PVA-PCL-NC nanofiber.

3.7. Antibacterial activity

3-7-1. Observation of the Antimicrobial Effect of Phage and Morphology and Classification of Bacteriophages

The specific lytic phage of *Escherichia coli* bacteria exhibited a robust antimicrobial effect by forming clear plaques in agar LB culture medium containing *E.coli* bacteria. These lysed spots on the culture medium surface were visually observed (Figure 8 a). The number of phages in

Journal Pre-proofs

the solution was quantified using Equation 1, resulting in an estimated titer of 10^{10} PFU/mL. After negative staining and examination of morphological characteristics using an electron microscope, the isolated bacteriophages were classified into the *Siphoviridae* and *Podoviridae* families (Figure 8b).

Ensuring the effective control and rapid identification of foodborne pathogens is crucial for ensuring food safety. Active packaging, incorporating films and antimicrobial substances, serves as a preventive measure to limit or reduce microbial growth on food surfaces. Bacteriophages, as natural antimicrobial agents, present a suitable option for food applications [51].

Figure 8: a) Escherichia coli bacteria undergoing lysis induced by bacteriophage. b) TEM microscope images of bacteriophages isolated from the coastal waters of the Caspian Sea, displayed (a. Belonging to the Siphoviridae family. b. Belonging to the Podoviridae family).

3-4. Observation of the Antimicrobial Activity of Active Electrospun Nanofibers from PVA, PCL, BNC Matrix, and Bacteriophage

The antimicrobial efficacy of electrospun nanofibers was assessed in MHA culture medium inoculated with *E.coli* at 37°C. The qualitative determination of the antimicrobial activity of immobilized phages against *Escherichia coli* was conducted by measuring the diameter of the inhibition zone. Electrospun nanofibers without phages (negative control) showed no inhibition zone, while the ampicillin disk (positive control) formed a 12-mm diameter zone. Active electrospun nanofibers, incorporating bacteriophages, exhibited a 13-mm diameter inhibition zone, indicating a specific lytic antimicrobial effect comparable to the antibiotic (Figure 9).

Figure 9. Represents the qualitative determination of the antimicrobial activity of immobilized phages against Escherichia coli by disc diffusion method.

3-5. Evaluation of Antimicrobial Ability of Phages Encapsulated in Nanofibers Over Time

After storing active nanofibers (with immobilized phages) and control samples (without phages) for one month at three temperatures (24°C, 4°C, and -20°C), their antimicrobial

Journal Pre-proofs

effectiveness was assessed. In a suspension containing 10^3 CFU/mL *Escherichia coli* bacteria, the remaining bacterial population was counted at 5-day intervals over 30 days. Control samples without phages showed no antimicrobial effect. Active nanofibers containing bacteriophages gradually lost antibacterial activity after one month at 24°C. However, nanofibers stored at 4°C and -20°C maintained their ability to lyse and destroy the target bacteria even after one month (Figure 10).

Figure 10: Results depicting the antimicrobial activity of electro-spun fibers a) without phage, b) with phage, over one month after storage at 24°C, 4°C, and -20°C. Data denote mean ± SD (n = 3); The value of P < 0.05 was considered statistically significant. ns = not significant (p > 0.05); *p ≤ 0.05; **p ≤ 0.01; ***p ≤ 0.001; ****p ≤ 0.0001., against multiple comparisons.

Bacteriophages exhibit characteristics akin to living organisms, including reproduction, genetic information, mutation, and evolution [52]. Combining bacteriophages with nanofibers facilitates the maintenance of their viability over extended periods. Nanofibers, acting as carriers for biological materials like bacteriophages, offer a promising avenue for combating bacterial infections [53]. Despite the challenges posed by the electrospinning technique, especially the high voltage involved, research suggests that encapsulating living cells, bacteriophages, and biological compounds within nanofibers is both feasible and advantageous.

Electrospinning, a specialized method for producing nanofibers, creates a network of polymeric nanofibers resembling a thin plastic layer. Incorporating biological products, sensitive to environmental factors, into nanofibers using electrospinning might seem challenging. However, various studies, including those encapsulating living cells, bacteriophages, and nucleic acids, demonstrate the feasibility and benefits of this approach. The rationale is to shield these biological entities from environmental factors, improve their quality and stability, and create flexible and practical materials through immobilization, drying, and freezing. Notably, nanofibers serve as effective carriers for medical treatments, offering protection, scaffolding for growth, and enhanced transfer capabilities. Natural and synthetic polymers,

Journal Pre-proofs

such as PEO, PVA, cellulose, and chitosan, have been employed to produce nanofibers encapsulating various biological agents, each offering specific advantages.

Previous studies have successfully demonstrated the antimicrobial effects of bacteriophages encapsulated in electrospun nanofibers. For instance, bacteriophage VB-Pae-Kakheti 25 capsid immobilized in electrospun PCL nanofibers exhibited antibacterial effects against Pseudomonas aeruginosa, a pathogen causing skin infections [54].

Similarly, bacteriophages T4, T7, and λ maintained their viability when enclosed in PVA nanofibers for over three months at sub-zero temperatures [55].

Furthermore, specific lytic phages isolated from wastewater and sewage samples demonstrated antimicrobial effects against *Escherichia coli*, forming plaques on culture mediums [56].

4. Conclusions

In conclusion, the development of active packaging incorporating bacteriophages presents a promising strategy for enhancing food safety by mitigating microbial contamination. This study investigated the fabrication, characterization, and functional properties of electrospun nanofiber mats containing bacteriophages for antimicrobial applications. The electrospinning process yielded defect-free fibers with random orientation, essential for consistent fiber dissolution and bacteriophage release. The resulting fiber mats exhibited uniformity in fiber diameter and morphology, with successful immobilization of bacteriophages within the matrix confirmed through electron microscopy. Chemical analysis confirmed the retention of polymer properties in the electrospun fibers, ensuring the integrity of the bioactive cargo. Mechanical testing demonstrated the isotropic nature of the fiber mats, with blends of PVA, PCL, and nanocellulose offering a balance between strength and flexibility. Further characterization revealed the hygroscopic nature of PVA-based fibers, while PCL exhibited hydrophobic behavior. Blending PVA and PCL modulated the surface properties, influencing moisture absorption and contact angle. However, the incorporation of nanocellulose minimally affected

Journal Pre-proofs

surface wettability. The study underscores the potential of electrospun nanofiber mats as effective carriers for bacteriophages, offering sustained release and antimicrobial activity. Future research should focus on optimizing fabrication parameters and evaluating the long-term stability and efficacy of bacteriophages within the nanofiber matrices.

Overall, the findings contribute to the advancement of active packaging technologies aimed at enhancing food safety and reducing the risk of foodborne illnesses through targeted antimicrobial interventions.

Acknowledgements:

The support of colleagues at the research center of Tabriz University of Medical Sciences Faculty of Nutrition and Health is acknowledged.

Founding source

This study was a part of Malahat Safavi Ph.D. thesis and financially supported by the Department of Food Industry Science and Technology, Faculty of Agriculture, University of Tabriz.

Data availability statement

The data that support the findings of this study are available from the corresponding author upon reasonable request.

Declaration of competing interest

All the authors of this article declare that they have no conflict of interest.

Journal Pre-proofs

[1] M. Nazari, H. Majdi, M. Milani, S. Abbaspour-Ravasjani, H. Hamishehkar, L.T. Lim, Cinnamon nanophytosomes embedded electrospun nanofiber: Its effects on microbial quality and shelf-life of shrimp as a novel packaging, Food Packaging Shelf Life 21 (2019).
[2] M. Xiao, J. Chery, M.W. Frey, Functionalization of Electrospun Poly(vinyl alcohol) (PVA) Nanofiber Membranes for Selective Chemical Capture, ACS Appl. Nano Mat. 1(2) (2018) 722-729.
[3] C. Ghosh, P. Sarkar, R. Issa, J. Haldar, Alternatives to Conventional Antibiotics in the Era of Antimicrobial Resistance, TRENDS MICROBIOL. 27(4) (2019) 323-338.
[4] S. Kumari, K. Harjai, S. Chhibber, Bacteriophage versus antimicrobial agents for the treatment of murine burn wound infection caused by Klebsiella pneumoniae B5055, J. Med. Microbiol. 60(2) (2011) 205-210.
[5] R.M. Dedrick, C.A. Guerrero-Bustamante, R.A. Garlena, D.A. Russell, K. Ford, K. Harris, K.C. Gilmour, J. Soothill, D. Jacobs-Sera, R.T. Schooley, G.F. Hatfull, H. Spencer, Engineered bacteriophages for treatment of a patient with a disseminated drug-resistant Mycobacterium abscessus, Nature Medicine 25(5) (2019) 730-733.
[6] D. Romero-Calle, R.G. Benevides, A. Góes-Neto, C. Billington, Bacteriophages as alternatives to antibiotics in clinical care, Antibiotics 8(3) (2019).
[7] H.Y. Shen, Z.H. Liu, J.S. Hong, M.S. Wu, S.J. Shiue, H.Y. Lin, Controlled-release of free bacteriophage nanoparticles from 3D-plotted hydrogel fibrous structure as potential antibacterial wound dressing, Journal of Controlled Release 331 (2021) 154-163.
[8] C. Zhou, R. Chu, R. Wu, Q. Wu, Electrospun polyethylene oxide/cellulose nanocrystal composite nanofibrous mats with homogeneous and heterogeneous microstructures, Biomacromolecules 12(7) (2011) 2617-2625.
[9] L. Meng, J. Li, X. Fan, Y. Wang, Z. Xiao, H. Wang, D. Liang, Y. Xie, Improved mechanical and antibacterial properties of polyvinyl alcohol composite films using quaternized cellulose nanocrystals as nanofillers, Compos. Sci. Technol. 232 (2023).
[10] A.S. Ribeiro, S.M. Costa, D.P. Ferreira, R.C. Calhelha, L. Barros, D. Stojković, M. Soković, I.C.F.R. Ferreira, R. Fangueiro, Chitosan/nanocellulose electrospun fibers with enhanced antibacterial and antifungal activity for wound dressing applications, React Funct Polym 159 (2021).
[11] Z. Jiang, B.T.D. Nguyen, J. Seo, C. Hong, D. Kim, S. Ryu, S. Lee, G. Lee, Y.H. Cho, J.F. Kim, K. Lee, Superhydrophobic polydimethylsiloxane dip-coated polycaprolactone electrospun membrane for extracorporeal membrane oxygenation, J. Membr. Sci. 679 (2023).
[12] K. Ahn, K. Park, K. Sadeghi, J. Seo, New Surface Modification of Hydrophilic Polyvinyl Alcohol via Predrying and Electrospinning of Hydrophobic Polycaprolactone Nanofibers, Foods 13(9) (2024).
[13] M.P. Doyle, J.L. Schoeni, Isolation of Escherichia coli O157:H7 from retail fresh meats and poultry, Appl. Environ. Microbiol. 53(10) (1987) 2394-2396.
[14] S.M. Horrocks, R.C. Anderson, D.J. Nisbet, S.C. Ricke, Incidence and ecology of Campylobacter jejuni and coli in animals, Anaerobe 15(1-2) (2009) 18-25.
[15] B. Molla, A. Mesfin, D. Alemayehu, Multiple antimicrobial-resistant Salmonella serotypes isolated from chicken carcass and giblets in Debre Zeit and Addis Ababa, Ethiopia, Ethiopian Journal of Health Development 17(2) (2003) 131-139.
[16] M. Meshkani, A. Mortazavi, Z. Pourfallah, Antimicrobial and physical properties of a chickpea protein isolate-based film containing essential oil of thyme using response surface methodology, Iranian Journal of Nutrition Sciences & Food Technology 8(1) (2013) 93-104.
[17] S. Hagens, M.J. Loessner, Bacteriophage for biocontrol of foodborne pathogens: Calculations and considerations, Curr. Pharm. Biotechnol. 11(1) (2010) 58-68.

Journal Pre-proofs

[18] H. Anany, W. Chen, R. Pelton, M.W. Griffiths, Biocontrol of Listeria monocytogenes and Escherichia coli O157:H7 in meat by using phages immobilized on modified cellulose membranes, Appl. Environ. Microbiol. 77(18) (2011) 6379-6387.
[19] B. Liu, S. Wu, Q. Song, X. Zhang, L. Xie, Two novel bacteriophages of thermophilic bacteria isolated from deep-sea hydrothermal fields, Curr. Microbiol. 53(2) (2006) 163-166.
[20] M. Salari, M. Sowti Khiabani, R. Rezaei Mokarram, B. Ghanbarzadeh, H. Samadi Kafil, Preparation and characterization of cellulose nanocrystals from bacterial cellulose produced in sugar beet molasses and cheese whey media, Int. J. Biol. Macromol. 122 (2019) 280-288.
[21] M. Salari, M. Sowti Khiabani, R. Rezaei Mokarram, B. Ghanbarzadeh, H. Samadi Kafil, Development and evaluation of chitosan based active nanocomposite films containing bacterial cellulose nanocrystals and silver nanoparticles, Food Hydrocolloids 84 (2018) 414-423.
[22] M. Ranjbar, A. Sharifan, S. Shabani, M. Amin Afshar, The Antimicrobial Effect of Garlic Extract on Staphylococous aureus and Escherichia coli O157: H7 in Ready to Cook Chicken, Journal of Food Technology and Nutrition 11(4) (2014) 57-66.
[23] J.M. Goddard, J.H. Hotchkiss, Polymer surface modification for the attachment of bioactive compounds, Prog Polym Sci (Oxford) 32(7) (2007) 698-725.
[24] M. Tolba, O. Minikh, L.Y. Brovko, S. Evoy, M.W. Griffiths, Oriented immobilization of bacteriophages for biosensor applications, Appl. Environ. Microbiol. 76(2) (2010) 528-535.
[25] A. Mahoutforoush, L. Asadollahi, H. Hamishehkar, S. Abbaspour-Ravasjani, A. Solouk, M.H. Nazarpak, Targeted Delivery of Pennyroyal via Methotrexate Functionalized PEGylated Nanostructured Lipid Carriers into Breast Cancer Cells; A Multiple Pathways Apoptosis Activator, Adv. Pharm. Bull. 13(4) (2023) 747-760.
[26] E. Vonasek, P. Le, N. Nitin, Encapsulation of bacteriophages in whey protein films for extended storage and release, Food Hydrocolloids 37 (2014) 7-13.
[27] F. Topuz, M.E. Kilic, E. Durgun, G. Szekely, Fast-dissolving antibacterial nanofibers of cyclodextrin/antibiotic inclusion complexes for oral drug delivery, Journal of Colloid and Interface Science 585 (2021) 184-194.
[28] E. Jamróz, P. Kulawik, P. Kopel, The effect of nanofillers on the functional properties of biopolymer-based films: A review, Polym. 11(4) (2019).
[29] T. Zheng, C.M. Clemons, S. Pilla, Grafting PEG on cellulose nanocrystals via polydopamine chemistry and the effects of PEG graft length on the mechanical performance of composite film, Carbohydr Polym 271 (2021).
[30] P. Singhaboot, W. Kraisuwan, T. Chatkumpjunjalearn, P. Kroeksakul, B. Chongkolnee, Development and Characterization of Polyvinyl Alcohol/Bacterial Cellulose Composite for Environmentally Friendly Film, J. Ecol. Eng. 24(6) (2023) 226-238.
[31] Y. Zhao, H. Sun, B. Yang, Y. Weng, Hemicellulose-based film: Potential green films for food packaging, Polym. 12(8) (2020).
[32] P. Panchal, E. Ogunsona, T. Mekonnen, Trends in advanced functional material applications of nanocellulose, Process. 7(1) (2019).
[33] T.M. Ejara, S. Balakrishnan, J.C. Kim, Nanocomposites of PVA/cellulose nanocrystals: Comparative and stretch drawn properties, SPE Polym. 2(4) (2021) 288-296.
[34] L. Meng, S. Ding, W. Li, D. Liu, E. Liu, Preparation and property analysis of cellulose reinforced carbon nanocomposite hydrogels, New J. Chem. 48(27) (2024) 12138-12145.
[35] H.M. Zidan, E.M. Abdelrazek, A.M. Abdelghany, A.E. Tarabiah, Characterization and some physical studies of PVA/PVP filled with MWCNTs, J. Mater. Res. Technol. 8(1) (2019) 904-913.
[36] X. Ji, J. Guo, F. Guan, Y. Liu, Q. Yang, X. Zhang, Y. Xu, Preparation of electrospun polyvinyl alcohol/nanocellulose composite film and evaluation of its biomedical performance, Gels 7(4) (2021).

Journal Pre-proofs

[37] Z. Chen, B. Wei, X. Mo, C.T. Lim, S. Ramakrishna, F. Cui, Mechanical properties of electrospun collagen-chitosan complex single fibers and membrane, Materials Science and Engineering C 29(8) (2009) 2428-2435.
[38] N. Bhardwaj, S.C. Kundu, Electrospinning: A fascinating fiber fabrication technique, Biotechnology advances 28(3) (2010) 325-347.
[39] H. Zhou, T.B. Green, Y.L. Joo, The thermal effects on electrospinning of polylactic acid melts, Polymer 47(21) (2006) 7497-7505.
[40] A. Azari, A. Golchin, M.M. Maymand, F. Mansouri, A. Ardeshirylajimi, Electrospun Polycaprolactone Nanofibers: Current Research and Applications in Biomedical Application, Adv. Pharm. Bull. 12(4) (2022) 658-672.
[41] A. Dufresne, Nanocellulose: A new ageless bionanomaterial, Mater. Today 16(6) (2013) 220-227.
[42] M.-J. Cho, B.-D. Park, Tensile and thermal properties of nanocellulose-reinforced poly (vinyl alcohol) nanocomposites, Journal of Industrial and Engineering Chemistry 17(1) (2011) 36-40.
[43] S. Palali, Cellulose Nanocrystals: Potential Replacement for Food Packaging, Science (July) (2019) 39-73.
[44] R.J. Moon, A. Martini, J. Nairn, J. Simonsen, J. Youngblood, Cellulose nanomaterials review: Structure, properties and nanocomposites, Chem. Soc. Rev. 40(7) (2011) 3941-3994.
[45] M.H. Rasheed, Q.S. Kadhim, A.A. Mohaimeed, R.J. Alsaedi, Synthesis and Evaluation Structural, Thermal and Electrical Properties for PCL/TiO2 Nanocomposites, Transactions on Electrical and Electronic Materials (2024) 1-11.
[46] D. Huang, Z.-D. Hu, Y. Ding, Z.-C. Zhen, B. Lu, J.-H. Ji, G.-X. Wang, Seawater degradable PVA/PCL blends with water-soluble polyvinyl alcohol as degradation accelerator, Polymer Degradation and Stability 163 (2019) 195-205.
[47] Y. Li, C. Han, Y. Yu, L. Xiao, Effect of loadings of nanocellulose on the significantly improved crystallization and mechanical properties of biodegradable poly (ε-caprolactone), Int. J. Biol. Macromol. 147 (2020) 34-45.
[48] R. Khoo, H. Ismail, W. Chow, Thermal and morphological properties of poly (lactic acid)/nanocellulose nanocomposites, Procedia Chemistry 19 (2016) 788-794.
[49] P. Gan, S. Sam, M.F.b. Abdullah, M.F. Omar, Thermal properties of nanocellulose-reinforced composites: A review, Journal of Applied Polymer Science 137(11) (2020) 48544.
[50] R. Korehei, J. Kadla, Incorporation of T4 bacteriophage in electrospun fibres, J. Appl. Microbiol. 114(5) (2013) 1425-1434.
[51] B. Wang, H. Wang, X. Lu, X. Zheng, Z. Yang, Recent Advances in Electrochemical Biosensors for the Detection of Foodborne Pathogens: Current Perspective and Challenges, Foods 12(14) (2023).
[52] S.T. Abedon, Bacteriophage Adsorption: Likelihood of Virion Encounter with Bacteria and Other Factors Affecting Rates, Antibiotics 12(4) (2023).
[53] T. Kielholz, F. Rohde, N. Jung, M. Windbergs, Bacteriophage-loaded functional nanofibers for treatment of P. aeruginosa and S. aureus wound infections, Scientific Reports 13(1) (2023).
[54] F. Nogueira, N. Karumidze, I. Kusradze, M. Goderdzishvili, P. Teixeira, I.C. Gouveia, Immobilization of bacteriophage in wound-dressing nanostructure, Nanomed. Nanotechnol. Biol. Med. 13(8) (2017) 2475-2484.
[55] W. Salalha, J. Kuhn, Y. Dror, E. Zussman, Encapsulation of bacteria and viruses in electrospun nanofibres, Nanotechnology 17(18) (2006) 4675-4681.
[56] M.M.S. Dallal, S.M. Imeni, F. Nikkhahi, Z. Rajabi, S.P. Salas, Isolation of E. Coli bacteriophage from raw sewage and comparing its antibacterial effect with ceftriaxone antibiotic, Int J Adv Biotechnol Res 7(3) (2016) 385-391.

Journal Pre-proofs

Fig1:

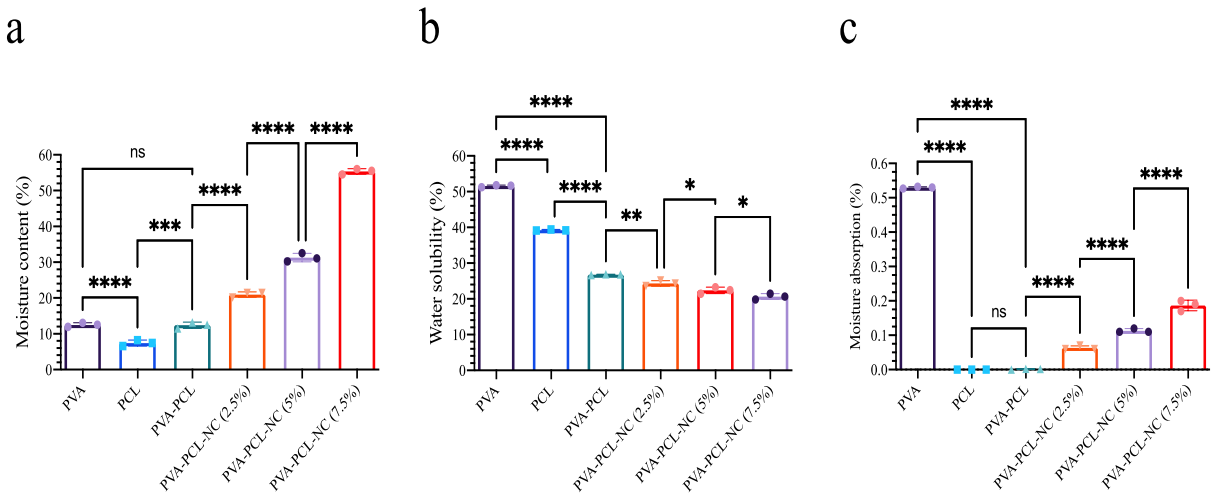

Journal Pre-proofs

Fig2:

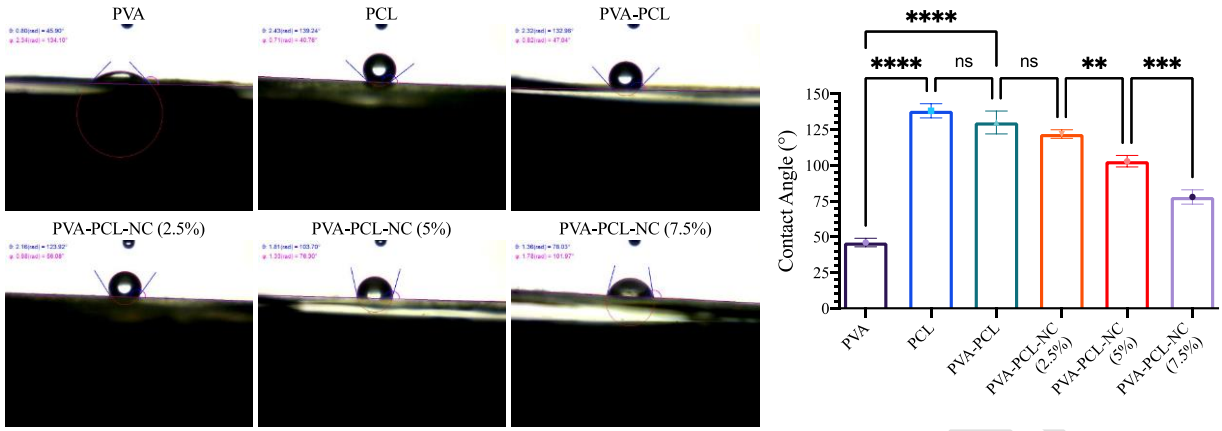

Journal Pre-proofs

Fig3:

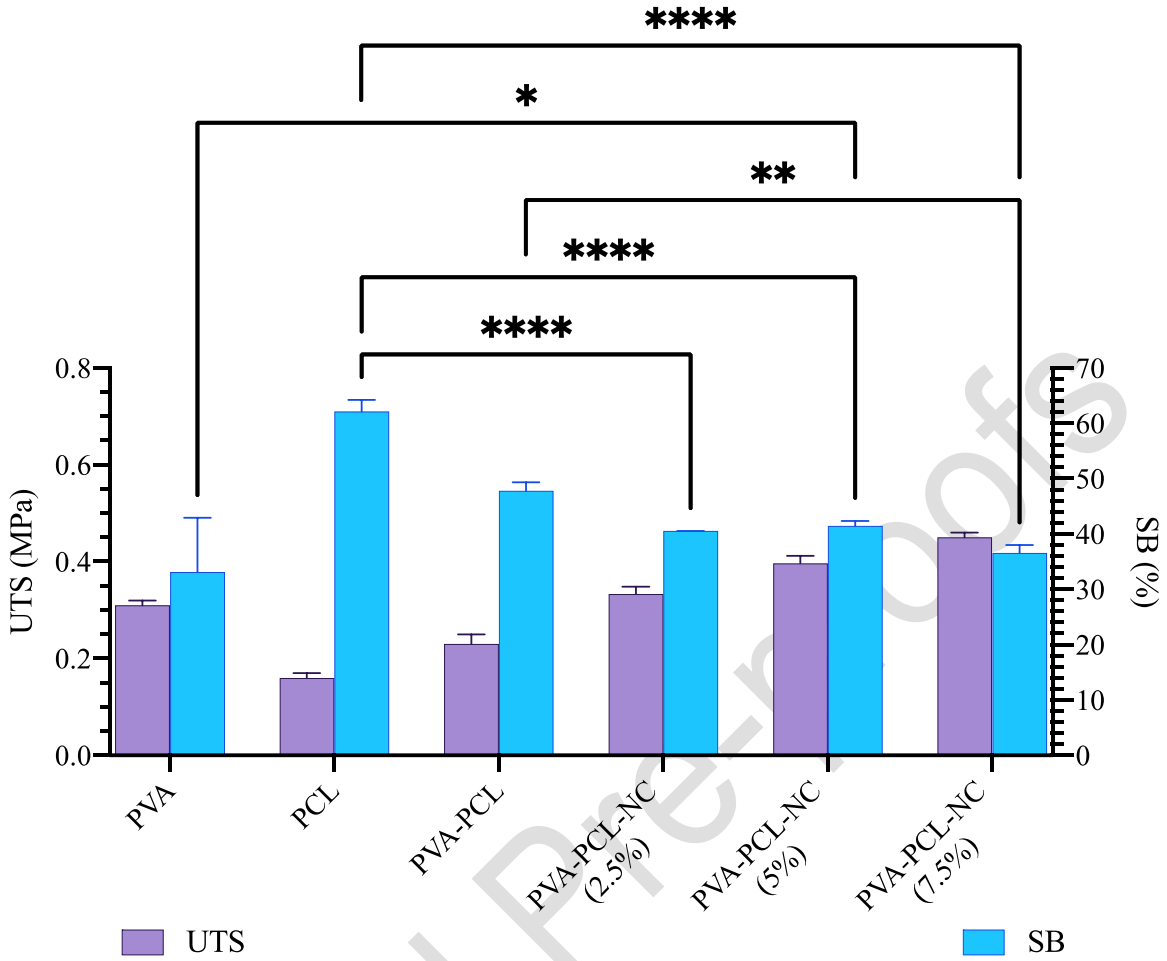

Journal Pre-proofs

Fig4:

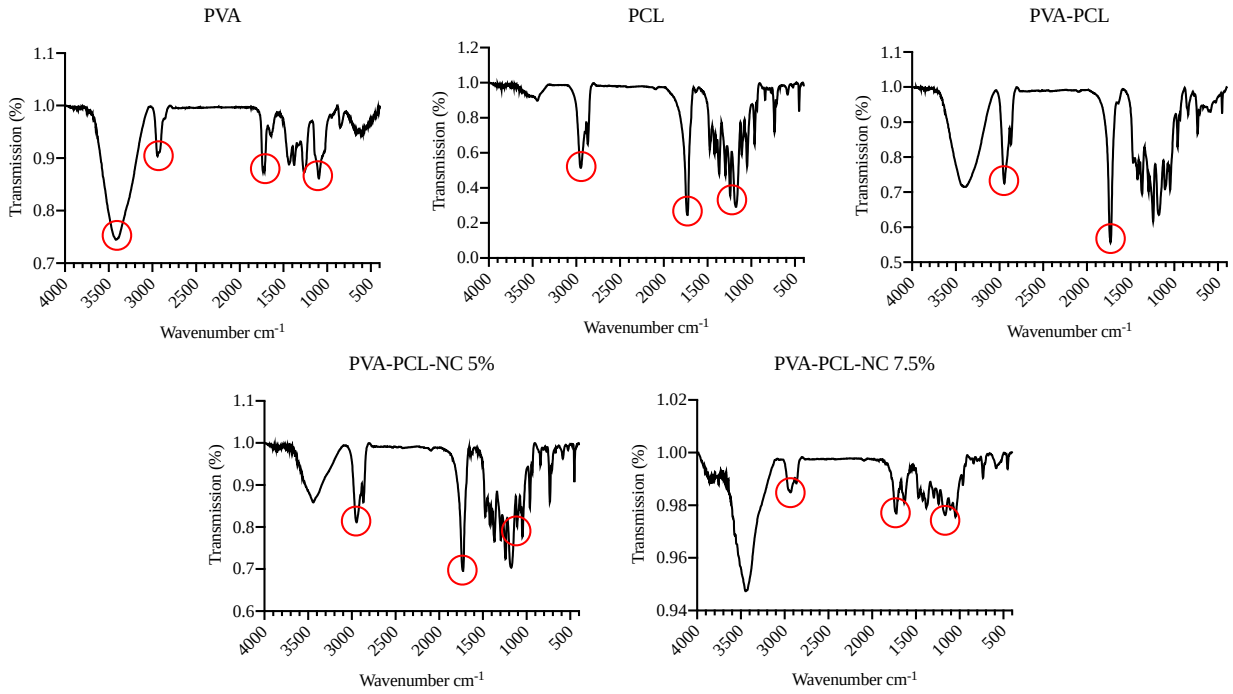

Journal Pre-proofs

Fig5:

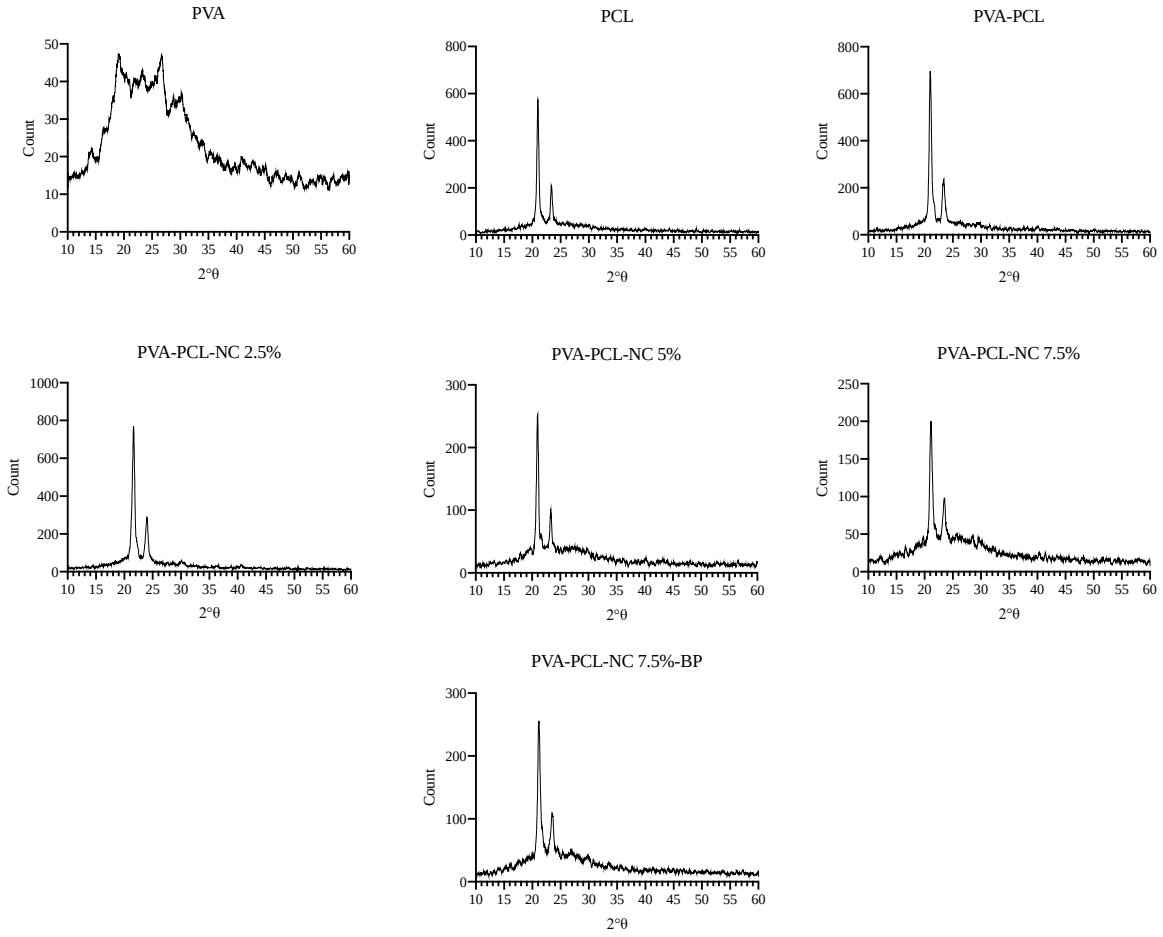

Journal

Fig6:

PVA

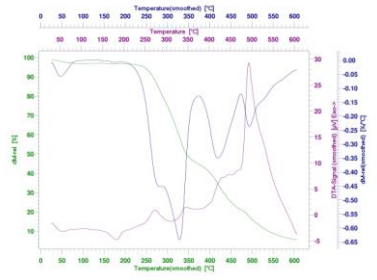

PCL

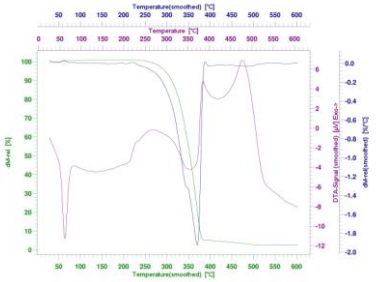

PVA-PCL

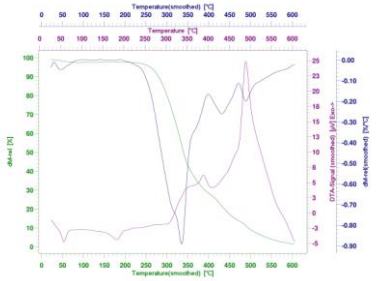

PVA-PCL-NC 2.5%

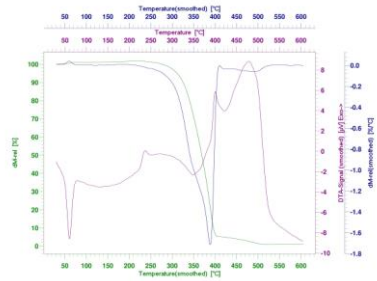

PVA-PCL-NC 5%

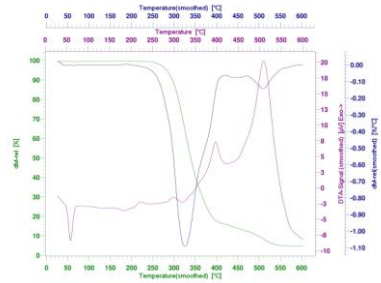

PVA-PCL-NC 7.5%

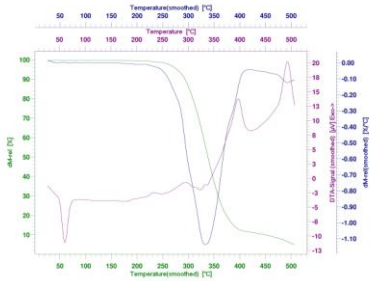

Journal Pre-proofs

Fig7:

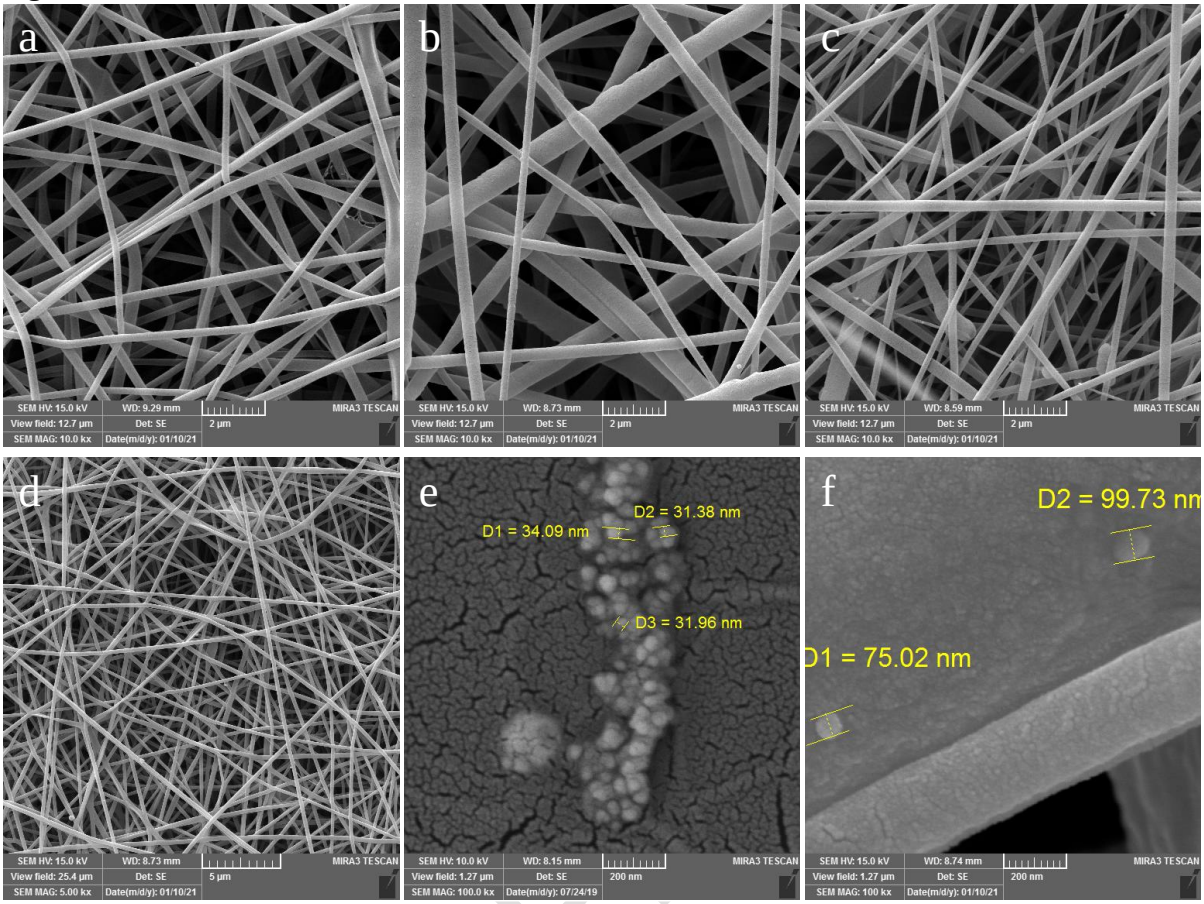

Journal Pre-proofs

Fig8:

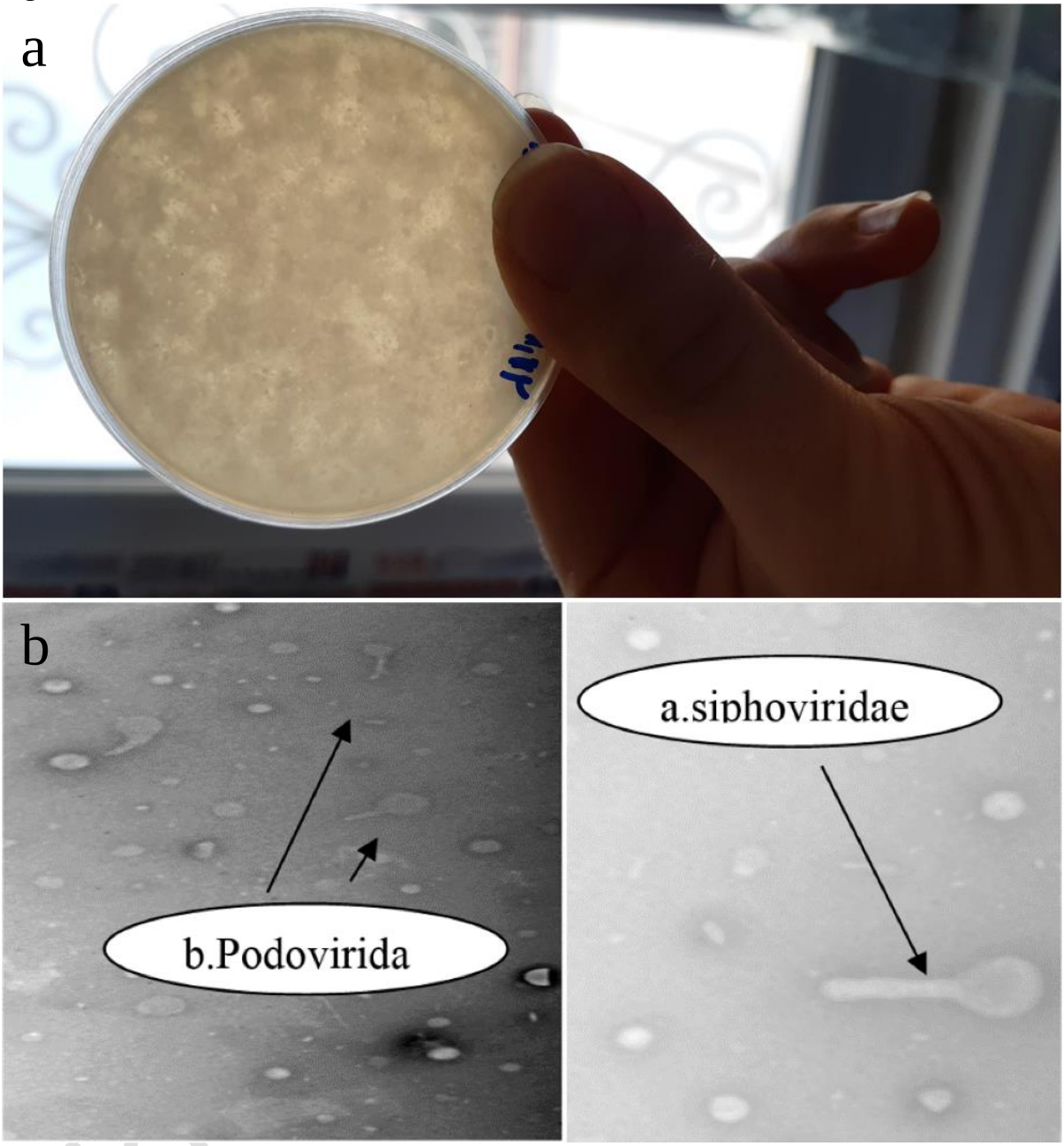

Fig9:

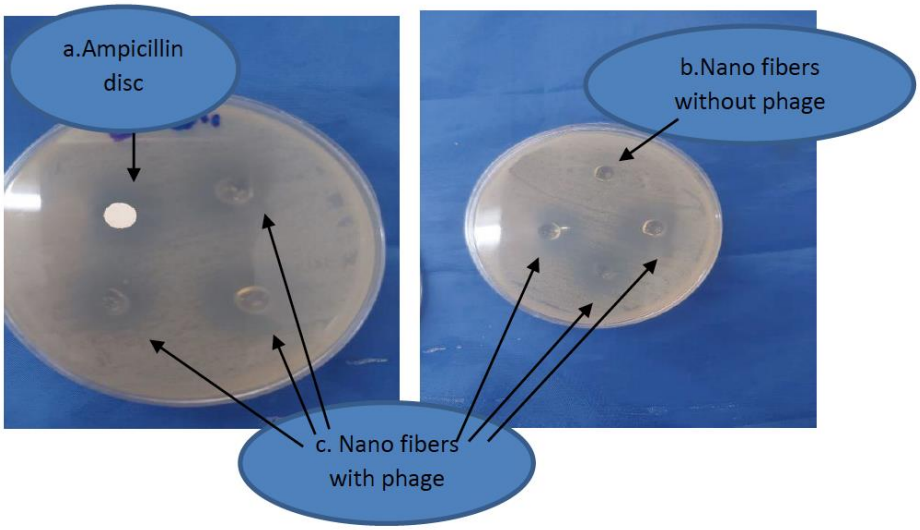

Journal Pre-proofs

Fig10:

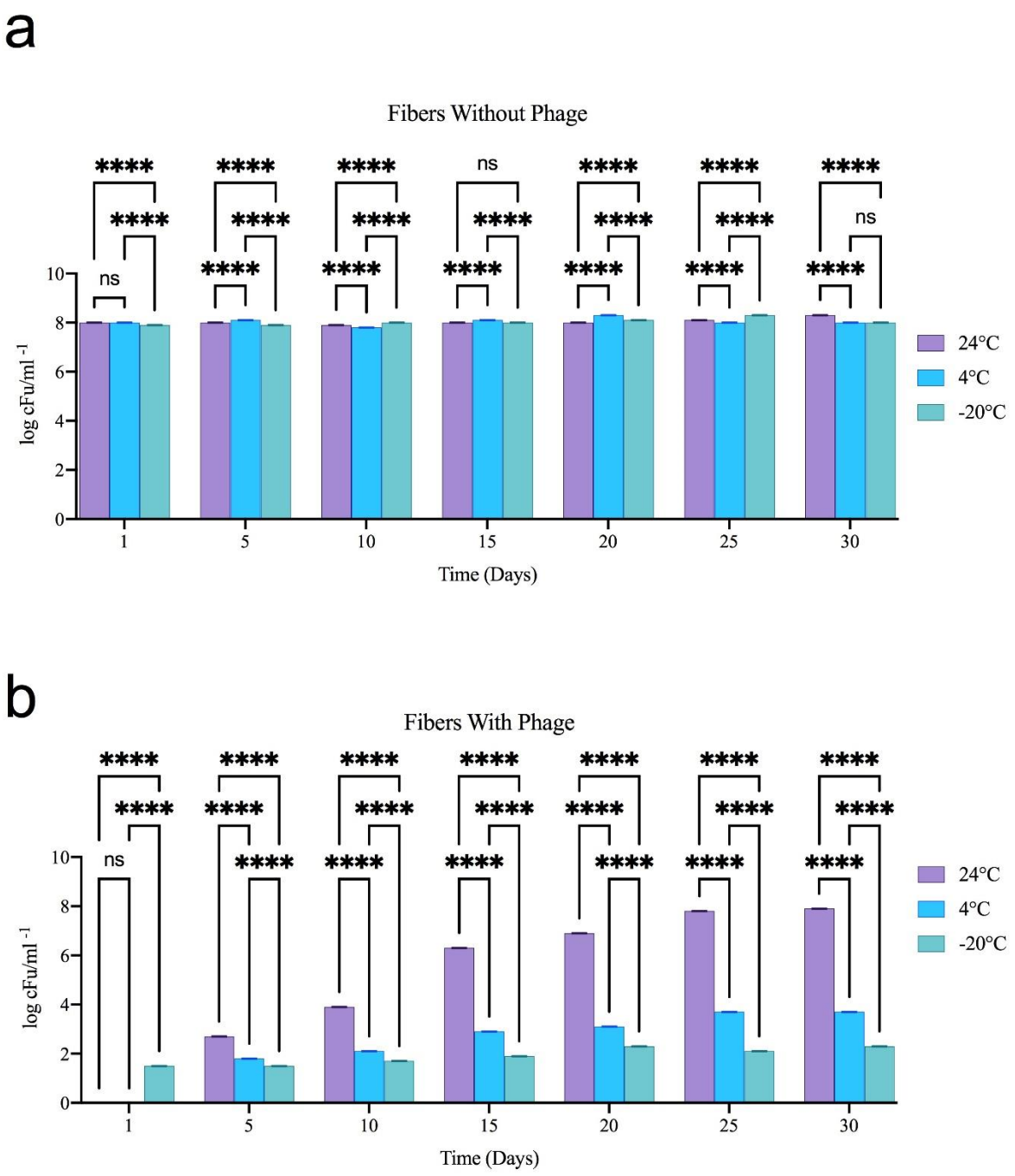
a
Fibers Without Phage
log cFu/ml -1
Time (Days)
24°C
4°C
-20°C
b
Fibers With Phage
log cFu/ml -1
Time (Days)
24°C
4°C
-20°C